American Journal of Applied Sciences

Original Research Paper

Double Diffusive Convection Heat and Moisture Transfer Inside a Planted Roof Building under Hot-Humid Climate: Case of Lomé City in West Africa

[1,2]Hodo-Abalo Samah, [2]Magolmèèna Banna and [3]Belkacem Zeghmati

[1]Department of Physics, Faculty of Sciences and Technologies, University of Kara, BP: 404, Kara, Togo
[2]Department of Physics, Faculty of Sciences, University of Lomé, BP: 1515, Lomé, Togo
[3]Department of Physics, University of Perpignan, Perpignan, France

Article history
Received: 17-09-2021
Revised: 06-12-2021
Accepted: 18-11-2021

Corresponding Author:
Hodo-Abalo Samah
Department of Physics, Faculty of Sciences and Technologies, University of Kara, BP: 404, Kara, Togo
Email: samah.abalo@gmail.com

Abstract: Planted roofs have been investigated as a passive cooling technology for energy efficiency purposes in buildings. More quantitative data on this topic are required to solve a lack of information for many specific regions. This study is focused on a numerical investigation of the thermal comfort inside a green roof rectangular ventilated cavity in a hot and humid climate like the one of Lomé in west Africa. The left vertical is heated and partly saturated with water to provide humidification of the indoor air. Transfer dimensionless equations are solved using an implicit finite difference scheme, the Thomas algorithm, and the Gauss-Seidel iterative method. We analyze the effects of inlet airflow on the thermal process inside the ventilated and planted enclosure have been investigated. The comfort temperature range deduced from the data is 25°C < T_c < 27°, and that of the indoor air humidity is 49% < Hr <60%. The different ranges obtained are significant and lead to improving inside thermal comfort. The solar flux of 350 W.m^{-2}, the average value in the case of Lomé city, was used to establish a heat transfer correlation to predict heat transfer through the roof with a relative error not exceeding 4%. This model can be very useful for engineers in the design and optimization stage of a green roof in practical buildings.

Keywords: Planted Roof, Heat and Mass Transfer, Leave-Area-Index, Modelling, Simulation

Introduction

Metallic and concrete roofs are very common in buildings in most developing countries and especially in tropical regions. Temperatures inside such buildings are usually above the comfortable range in these regions. Direct cooling devices electrically operated are feasible but are expensive and exposed to unreliable electrical grids. In such a context, passive cooling techniques seem more appropriate to provide comfort. Passive cooling in buildings includes roofs treated with thermal insulation, painted with white paint, shallow pond with thermal insulation, and evaporative cooling (Nahar *et al*., 1999; Jain, 2006; Joseph, 1999; Tang and Etzion, 2004). One way is to consider any treatment of the building which reduces its cooling load, such as solar control and minimizing internal heat gains. Studies in the literature show that a great part of the heat gains inside a building is brought about by roof elements (Nahar *et al*., 1999). In hot-humid climates, some methods or techniques are better adapted to improve thermal comfort in buildings. Particularly, the use of thermal insulation underneath and above the concrete flagstone roof reduces the heat load in a building (Samah and Banna, 2009; Banna *et al*., 2002; Del Barrio, 1998). In literature, approaches and research findings regarding the role of green roofs in urban heat mitigation and improving thermal comfort in buildings can be found. A literature review confirms the advantage of green roofs and their potential for reducing the intensity of heat islands and excess heat in building in different climatic zones (Jamei *et al*., 2021; Hodo-Abalo *et al*., 2012; Dong *et al*., 2020; Samah *et al*., 2020). Green roof performance is associated with a physical process like evapotranspiration and shading (Kumar and Kaushik, 2005) that contributes fairly well to energy efficiency in buildings and urban heat island mitigation (Wong *et al*., 2003).

Nowadays, controlling the indoor air environment is an essential asset for the study of double-diffusive mixed

convection in a ventilated room. In a ventilated cavity there can be two different types of convection; in particular, the natural internal convection induced by the buoyancy forces thanks to the heat and mass sources and the external convection forced by mechanical ventilation. The fluid flow structure and the dynamics of heat or mass transfer within the ventilated cavity are governed by the interaction between natural and forced convections resulting in diffusive mixed double convection. In a literature review, studies have shown interest in the problem of mixed convection in rectangular ventilated enclosures. Thus, Angirasa (2000) and Raji and Hasnaoui (1998) carried out a numerical study of laminar mixed convection in a two-dimensional enclosure subjected to an auxiliary or contrary jet with a heated side wall. Mixed convection in ventilated cavities where the horizontal top wall and the left vertical wall were subjected to equal heat fluxes has been studied by Raji and Hasnaoui (2000). However, the effects of thermal and mass buoyancy forces induced by temperature and concentration gradients have not been sufficiently investigated. Yan (1996) and Lee *et al*. (1997) analyzed by laminar mixed convection, the transport phenomena in heat and mass transfers in conduits.

When considering green roof building cavities, the effect of foliage material on flow structure is poorly known. Some experimental studies have been reported on thermal performance but few models exist for practical building optimization. A green roof as a passive cooling technique requires detailed studies to increase the amount of reliable data that can support its dissemination (Sailor *et al*., 2008). Indeed, climatic conditions play an important role in the behavior of green roofs. Thus, quantitative data in the context of hot and humid tropical climates are still needed. The research conducted had the following objectives:

- To propose a heat transfer model for a green roof under the hot and humid climate of Lomé city in west Africa
- To analyze the effect of foliage density on the temperature and humidity field and inside fluid flow characteristics
- To evaluate the potential improving thermal comfort inside a green roof building

The model can be very useful for engineers in the design and optimization stage of a green roof in practical buildings.

Modeling and Numerical Procedure

Physical Model

The physical model consists as can be seen in Fig. 1 of a ventilated rectangular cavity with inlet and outlet openings on their vertical walls. The inlet opening of size *e* is located on the bottom of the vertical wall allowing the ambient airflow to get in at a uniform velocity. The warm air from the cavity is discharged through the outlet opening placed at the top of the left vertical wall. The inlet and outlet opening has the same size. The green roof is composed of a layer of flagstone of thickness equal to 20 cm surmounted by a layer of soil (30 cm of thickness) and a canopy. The heat flux transferred into the cavity through the top wall comes from the green roof while the left vertical wall is saturated with water and heated. Other walls are assumed adiabatic. Besides, solid walls are supposed to be impermeable.

Mathematical Model

In this study, the green roof model is characterized by the solar heat gain Factor (FE) used to calculate the heat flux transferred to the cavity through the green roof. Previous studies (Hodo-Abalo *et al*., 2012) have proposed a correlation to calculate the EF according to the Leaf Area Index (LAI):

$$FE = \kappa \exp\left(-\frac{LAI}{\pi}\right) + \vartheta \tag{1}$$

where:

$$\kappa = 97.48257 \exp\left(-\frac{B_o}{3.27898}\right) + 8.07878$$

$$\pi = -0.19839 + 0.19839 + 0.14606 Bo - 0.00693 Bo^2 + 0.00021 Bo^3 - 2.916210^{-6} Bo^4 \vartheta = 1.98266$$

B_o = The biot number

Transfer equations have been presented for double diffusion mixed convection and completed by the boundary conditions.

The following assumptions are made in the analysis:

- The laminar airflow is two dimensional
- Fluids are incompressible and isotropic
- Thermophysical properties of the fluids are assumed to be constant except for the density which obeys the Boussinesq approximation
- Viscous heat dissipation is neglected

Considering these simplifying assumptions, the dimensionless equations are written using the stream function and vorticity formulation. Dimensionless variables are chosen as follows:

$$U = \frac{u}{u_0} V = \frac{v}{u_c} = \tau = \frac{tu_0}{H} X = \frac{x}{H} Y = \frac{Y}{H}$$

$$\Omega = \frac{\omega H}{u_0} \Theta + = \frac{\lambda\left(T - T_\partial\right)}{\phi(FE)H} C^* = \frac{pL_V D\left(C - C_\partial\right)}{\xi \phi H} \tag{2}$$

$$B_1 = \frac{e}{H} B_2 = \frac{H - e}{H}$$

DOI: 10.3844/ajassp.2022.6.20

With these dimensionless variables, vorticity, heat, and mass transfer equations inside the enclosure are:

$$\frac{\partial \Omega}{\partial \tau}+U\frac{\partial \Omega}{\partial X}+V\frac{\partial \Omega}{\partial Y}=\frac{1}{R_e}\left(\frac{\partial^2 \Omega}{\partial X^2}+\frac{\partial^2 \Omega}{\partial Y^2}\right)+R_{iT}\left(\frac{\partial \Theta}{\partial X}\right)+R_{iS}\left(\frac{\partial C^*}{\partial X}\right) \tag{3}$$

$$\frac{\partial^2 \Psi}{\partial X^2}+\frac{\partial^2 \Psi}{\partial Y^2}+\Omega=0 \tag{4}$$

$$\frac{\partial \Theta}{\partial \tau}+U\frac{\partial \Theta}{\partial X}+V\frac{\partial \Theta}{\partial \gamma}=\frac{1}{P_\gamma R_e}\left(\frac{\partial^2 \Theta}{\partial X^2}+\frac{\partial^2 \Theta}{\partial Y^2}\right) \tag{5}$$

$$\frac{\partial C^*}{\partial \tau}+U\frac{\partial C^*}{\partial X}+V\frac{\partial C^*}{\partial X}=\frac{1}{S_C R_e}\left(\frac{\partial^2 C^*}{\partial X^2}+\frac{\partial^2 C^*}{\partial Y^2}\right) \tag{6}$$

The dimensionless numbers such as Prandtl number, Schmidt number, Reynolds number, thermal Grash of number, solutal Grash of number, thermal Richardson number, and solutal Richardson number are defined as follows:

$$P_\gamma=\frac{\nu}{\alpha},S_C=\frac{\nu}{D},R_e=\frac{u_0 H}{\nu},G_{\gamma T}=\frac{g\beta_T H^4(FH)\phi}{\lambda \nu^2},$$
$$G_{\gamma S}=\frac{g\beta_C H^4 \zeta\phi}{pL_v D\nu^2},R_{iT}=\frac{G_\gamma T}{R_e^2},R_{iS}=\frac{G_{\gamma S}}{R_e^2} \tag{7}$$

As defined, it is clear that the thermal Grash of number is a function of LAI. Temperature, water vapor density, velocity, vorticity, and stream function are initialized as follows:

$$U=V=0\ \ \psi=0,\Omega=0,\Theta=0,C^*=0 \tag{8}$$

The following boundary conditions are used to complete the above equations:

- Inlet: $X=0,0\le Y\le B_1$:

$$U=1,V=0,\psi=Y,\Omega=0,\Theta=0, \tag{9}$$

- Outlet: $X = L/H$, $B_2 \le Y \le 1$:

$$\left.\frac{\partial U}{\partial X}\right|_{X=L/H}=\left.\frac{\partial V}{\partial X}\right|_{X=L/H}=0, \tag{10}$$

$$\left.\frac{\partial \Theta}{\partial X}\right|_{X=L/H}=\left.\frac{\partial^2 \Psi}{\partial X^2}\right|_{X=L/H}=0, \tag{11}$$

$$\left.\frac{\partial \Theta}{\partial X}\right|_{X=L/H}=\left.\frac{\partial C^*}{\partial X}\right|_{X=L/H}=0 \tag{12}$$

- On the heated and saturated left wall:

$$X=0,B_1\le Y\le 1$$
$$U_d=-\frac{q}{u_0 pL_V}\left.\frac{\partial C^*}{\partial X}\right|_{X=0},V=0 \tag{13}$$

$$\Psi=U_d Y,\Omega=-\left.\frac{\partial^2 \psi}{\partial X^2}\right|_{X=0}, \tag{14}$$

$$-\frac{SHF}{\zeta}\left.\frac{\partial \Theta}{\partial X}\right|_{X=0}-\left.\frac{\partial C^*}{\partial X}\right|_{X=0}=1 \tag{15}$$

where ξ is the ratio of the heat transmitted to the wetted wall:

- On the top heated wall:

$$Y=1,0\le X\le L/H,U=V=0,$$
$$\left.\frac{\partial \Psi}{\partial \gamma}\right|_{Y=1}=0,\Omega=-\left.\frac{\partial^2 \Psi}{\partial \gamma^2}\right|_{Y=1} \tag{16}$$

$$\left.\frac{\partial \Theta}{\partial \gamma}\right|_{Y=1}=1,\left.\frac{\partial C^*}{\partial \gamma}\right|_{Y=1}=0\ , \tag{17}$$

- Other walls are impermeable and adiabatic:

$$U=V=0,\psi=0,\Omega=-\frac{\partial^2 \psi}{\partial n^2} \tag{18}$$

$$\frac{\partial C^*}{\partial n}=\frac{\partial \Theta}{\partial n}=0 \tag{19}$$

The relative humidity is deduced as a ratio of the vapor pressure P_V and the saturated vapor pressure P_{Vs} used (Tiwari, 2002).

The average Nusselt and Sherwood numbers are used to describe heat and mass transfer rates respectively:

- On the top wall:

$$Nu_{av}=\int_0^1 \frac{N_{u1}(X)}{n}dX \tag{20}$$

where local Nusselt is calculated as follows:

$$N_{u1}(X)=\left.\frac{1}{\Theta}\right|_{y=1} \tag{21}$$

- On the left wall

Local Nusselt and Sherwood numbers are calculated as follows:

$$N_{u2}(Y)=\left.\frac{1}{c^*}\right|_{X=1} \tag{22}$$

$$S_C(Y)=\frac{1}{c^*}\Big|_{X=0} \quad (23)$$

Numerical Procedure

The implicit finite difference method was used to discretize the transfer equations. The diffusive terms were approximated using the central finite difference scheme. The system of algebraic equations obtained is solved using the Thomas algorithm and the Gauss-Seidel iterative method. The time and spatial steps retained for this study are respectively Δt = 0.0025 and ΔX = 0.0025 m, ΔY = 0.0025 m. Fig. 2 is shown the methodology flowchart retained for the study. The initial data (solar flux density, leaf area index, ambient temperature, etc.,) is considered as input to solve different equations. An iterative process was applied and the following criterion was used to assess the convergence of the solution:

$$\left|\left(x_{i,j}^{k+1}-x_{i,j}^{k}\right)/x_{i,j}^{k}\right|\leq 10^{-5} \quad (24)$$

where, $x is \Theta, C^*, \Psi or \Omega$.

Mesh Refinement and Code Validation

The size of the grid has been optimized to make the results independent of the chosen size. The optimized 81 × 81 grid was retained for the calculations in this study. We tested our algorithm on the problem of Saha *et al*. (2009) to verify the accuracy of our numerical procedure and the comparison of the results shows a satisfactory agreement. Indeed, similar distributions of streamlines, isotherms and concentrations are obtained. In Fig. 3, are shown our results obtained by our procedure and those of Sumon for P_r = 0.7, R_e = 100, R_i = 10, and buoyancy ratio N = 1. Our procedure was also tested on the problems of Vahl Davis (1983), Manzari (1999), and Wan *et al.* (2001) with a satisfactory agreement as shown in Table 1. The code developed in Formula Translation (FORTRAN) and validated, is applied to the simulation of the present model.

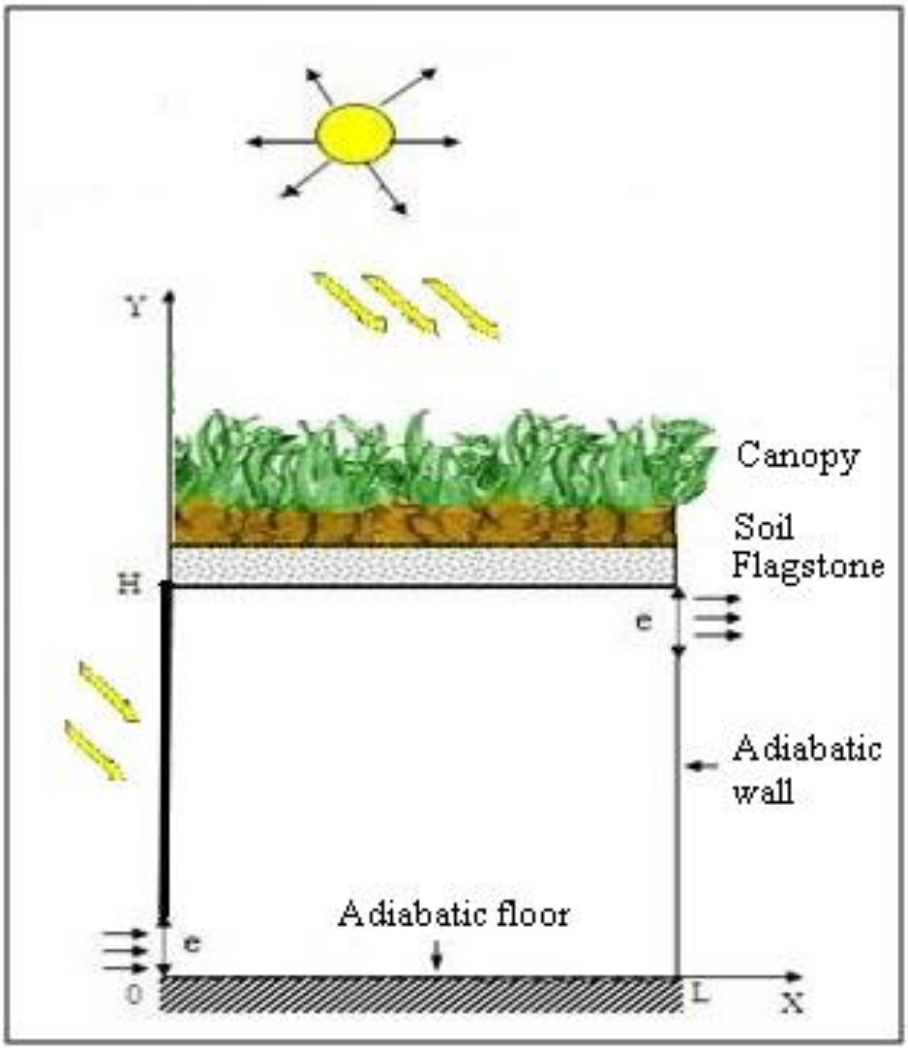

Fig. 1: Adopted physical model

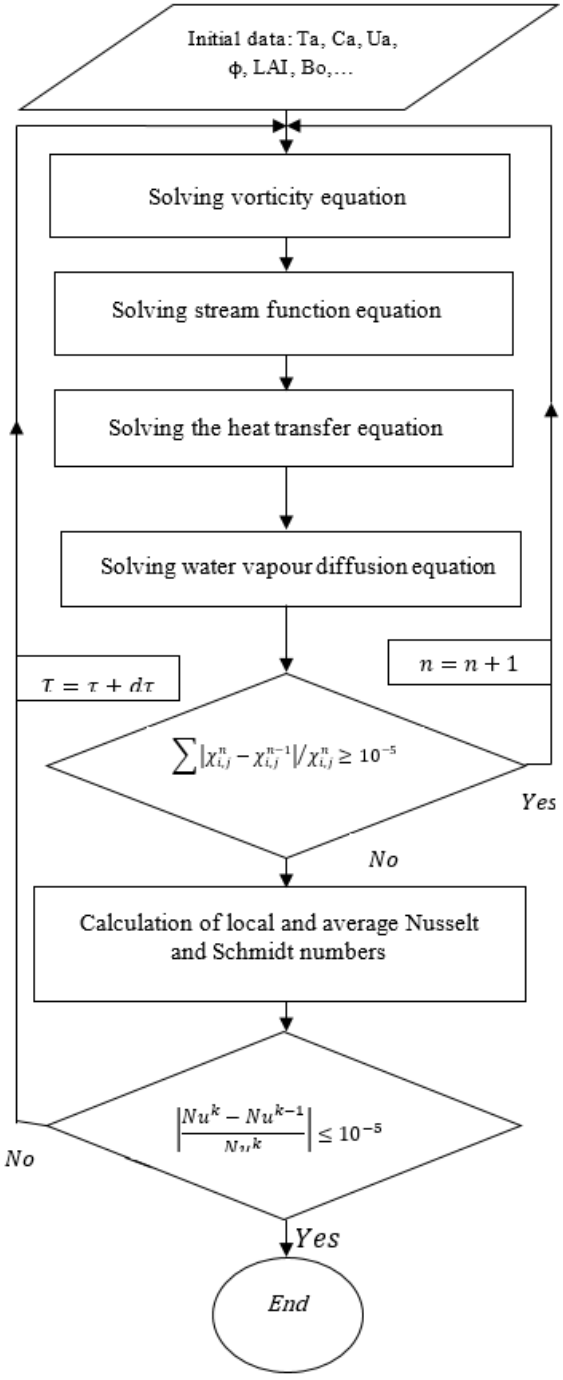

Fig. 2: Methodology flowchart used in the present study

Main Results and Analysis

The dimensions of the ventilated enclosure, inlet, and outlet openings are taken constantly as, $B_1 = 0.1$ and $B_2 = 0.9$. The mixed convective study was carried out for the Prandtl number $Pr = 0.72$. Reynolds number is calculated by incrementing the air velocity at the entrance of the cavity while the music or solutal Grash of number is obtained from solar irradiation. Solar irradiation used for computation in this study is an average value illustrating solar irradiation in different selected localities. Particular attention is paid to Lomé climate conditions which are described by some meteorological parameters which we have plotted in Fig. 4. In this case, ϕ value is equal to 350 W.m^{-2} on average. The thermal Richardson or Grash of numbers according to its definition in this study, strongly depends on the LAI. Therefore, the leaf area index is chosen as the main sensitivity parameter of the model. Particular attention is paid to its effects on the flow structure. The LAI values considered for this simulation are in the range one and six. This study examines the heat transfer and fluid flow characteristics induced by mixed convection with a constant heat source at the horizontal top wall which represents the green roof and a mass source at the left vertical wall. The resulting flow structure is analyzed to provide a fundamental understanding of the effect of the LAI and Re on flow, but also on temperature and water vapor concentration fields. In the present study, Nusselt and Sherwood numbers were important dimensionless parameters in heat and mass transfer description. Effects of the LAI and Reynolds number on those parameters have been examined.

Characteristics of Flow Structure, Temperature, and Mass Concentration Fields

Streamline, isotherms, and concentration lines are used to describe mixed convection with heat and mass transfer in the ventilated cavity. A study of the sensitivity of the Nusselt and Sherwood numbers to the main parameters was presented and discussed. Streamline, isothermal, and concentration contours illustrating the effect of the Leaf Area Index are presented in Fig. 5-7 for different solar radiation heat fluxes. The flow structure is characterized by open lines and fluid recirculation at the bottom. The effect of natural convection remains present but relatively weak at high LAI values as the open lines characterizing forced convection remain slightly dominant as shown in Fig. 5a, 6a, and 7a. For a given value of ϕ, an increase in LAI decreases the Richardson number.

A decrease in LAI (increased Richardson number) causes a gradual development of the recirculation cells in the lower right corner of the cavity thus causing a change in the flow structure. For lower values of ϕ, there is competition between imposed airflow and the natural convection as illustrated by the streamlines in Fig. 5a. At higher ϕ values (streamlines of Fig. 7a), the lower recirculation cells spread and lessen the induced flow and at the same time result in substantially the same kinetic energy in the induced flow practically equivalent to that of the inlet section. Heat transfer by convection induces the growth of recirculating cells and

induces faster removal of heat and water vapor from heat and mass sources. The increase in heat flow and concentration gradients induces an increase in buoyancy forces. Recirculation cells grow by absorbing thermal energy through induced forced flow. Thus, the compressed forced flow covers the heat and mass sources at low LAI values. The shifting of the isothermal, is concentration, and is humidity fronts throughout the cavity characterizes the temperature and water vapor fields and shows the effect of natural convection on the distribution of these fields. Since the induced flow sweeps overheat and mass level to the upper left corner of the cavity decrease indicating better heat and mass transfer. As the Richardson number increases, the non-linearity of the different fields increases and the appearance of the plume is real and indicates the establishment of a double-diffusive flow of natural convection. In this case, the thermal conduction in the fluid becomes predominant (isotherm lines of Fig. 6b and 7b).

The heat transfer characteristic has been expressed by the Nusselt heat transfer number. For different LAI values and a given solar heat flux value, variations of the Nusselt number on the rooftop are examined. Results showed that an increase of LAI gradually decreases the Nusselt numbers towards a limit value as shown in Fig. 8. The effect of the Leaf Area Index on Nusselt number for different solar heat flux values is presented in Fig. 9. The evolution of the Nusselt number showed clearly that, it decreases as LAI increases. On other hand, heat transfer from the planted roof is significantly reduced with a very dense vegetation canopy on the rooftop and the thermal quality in the enclosure can be improved. This result is in good agreement with that of the previous study, which proved that heat transfer across a planted roof decreases as LAI increases (Hodo-Abalo *et al*., 2012). Heat transfer is affected by the flow structure taken into account with the Reynolds number. Nusselt number as a function of LAI increases with Reynolds number as shown in Fig. 10. The phenomenon not only intensified heat transfer but also increases the quantity of heat-driven out of the enclosure.

DOI: 10.3844/ajassp.2022.6.20

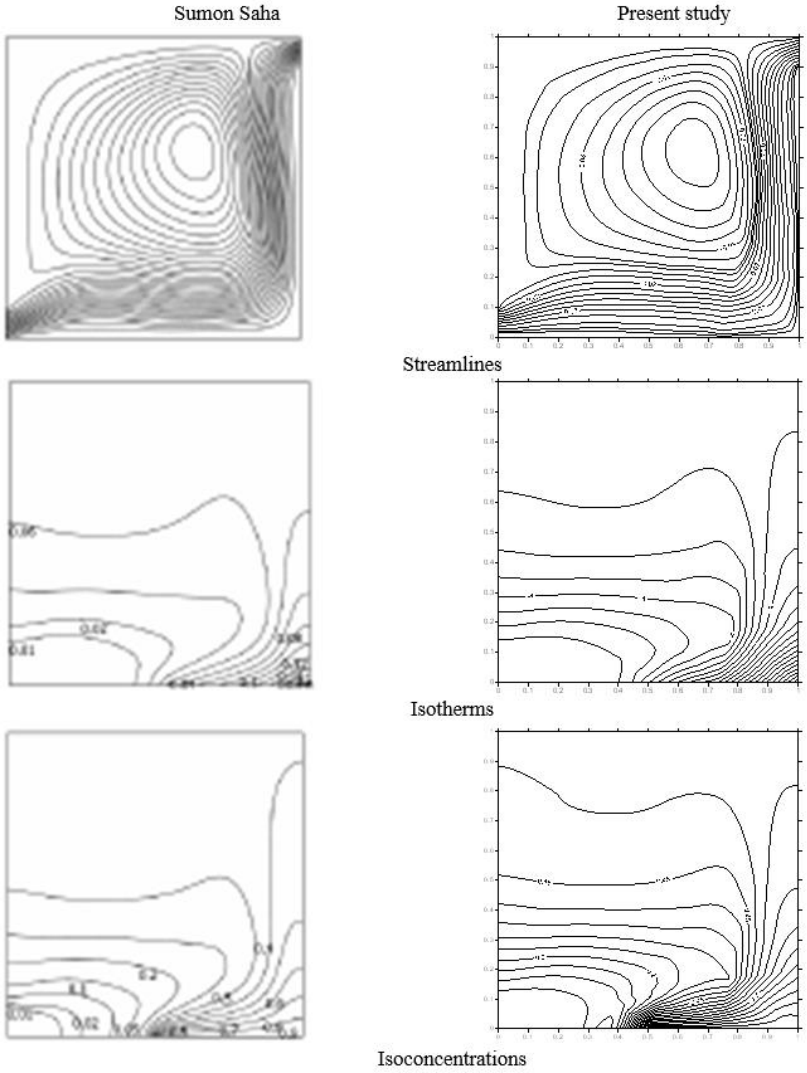

Fig. 3: Validation (Saha *et al*., 2009)

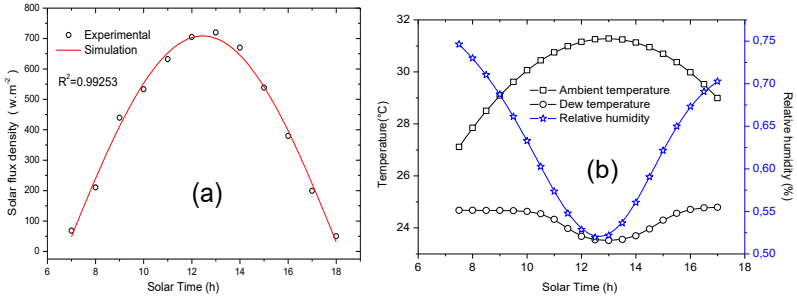

Fig. 4: Some meteorological parameters: (a) Solar irradiation; (b) ambient and dew temperatures, relative humidity

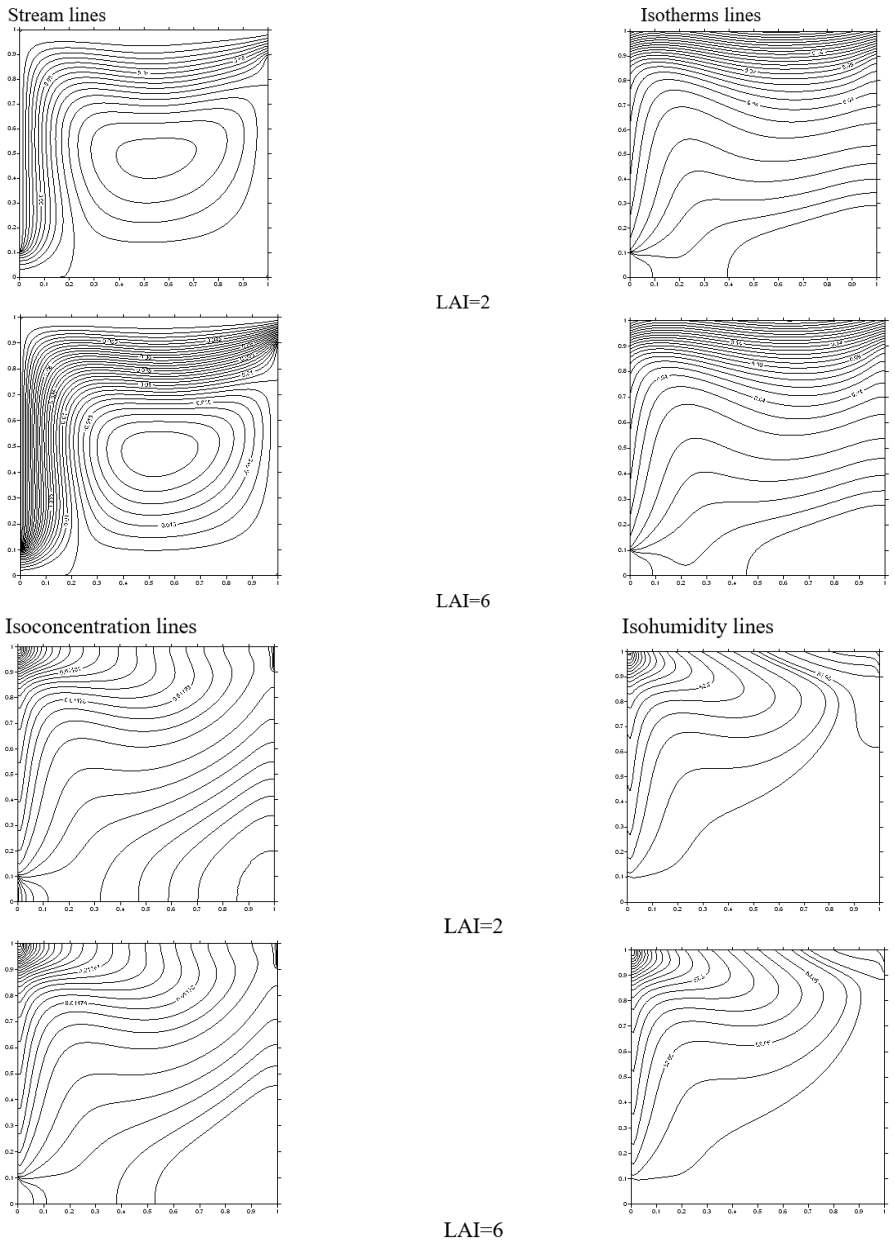

Fig. 5: (a) Streamlines and isotherm lines for $\phi = 50$ W/m^2; (b) is concentration lines and is humidity lines for $\phi = 50$ W/m^2

DOI: 10.3844/ajassp.2022.6.20

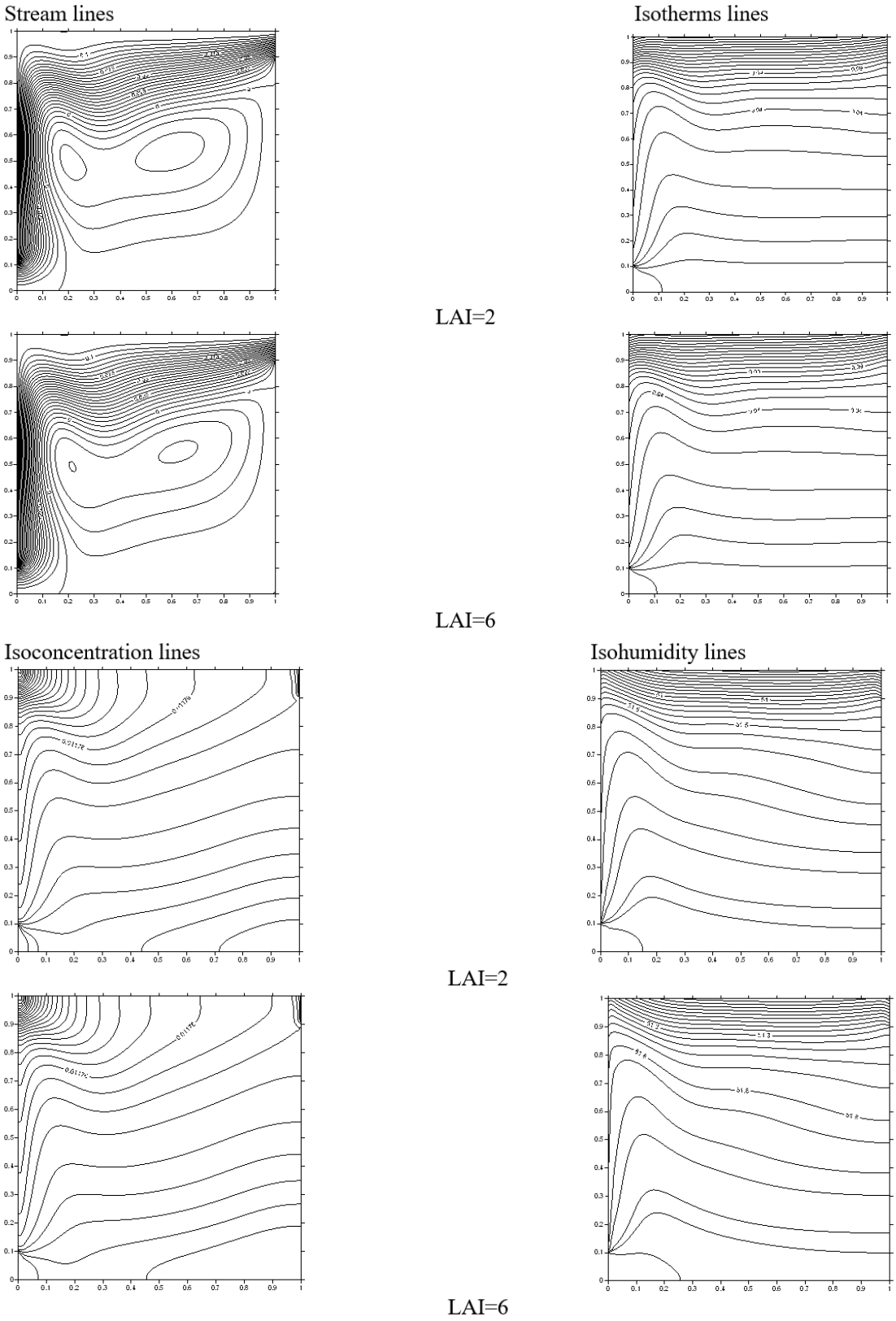

Fig. 6: (a) Streamlines and isotherm lines for ϕ=100 W/m^2; (b) is concentration lines and is humidity lines for ϕ = 100 W/m^2

DOI: 10.3844/ajassp.2022.6.20

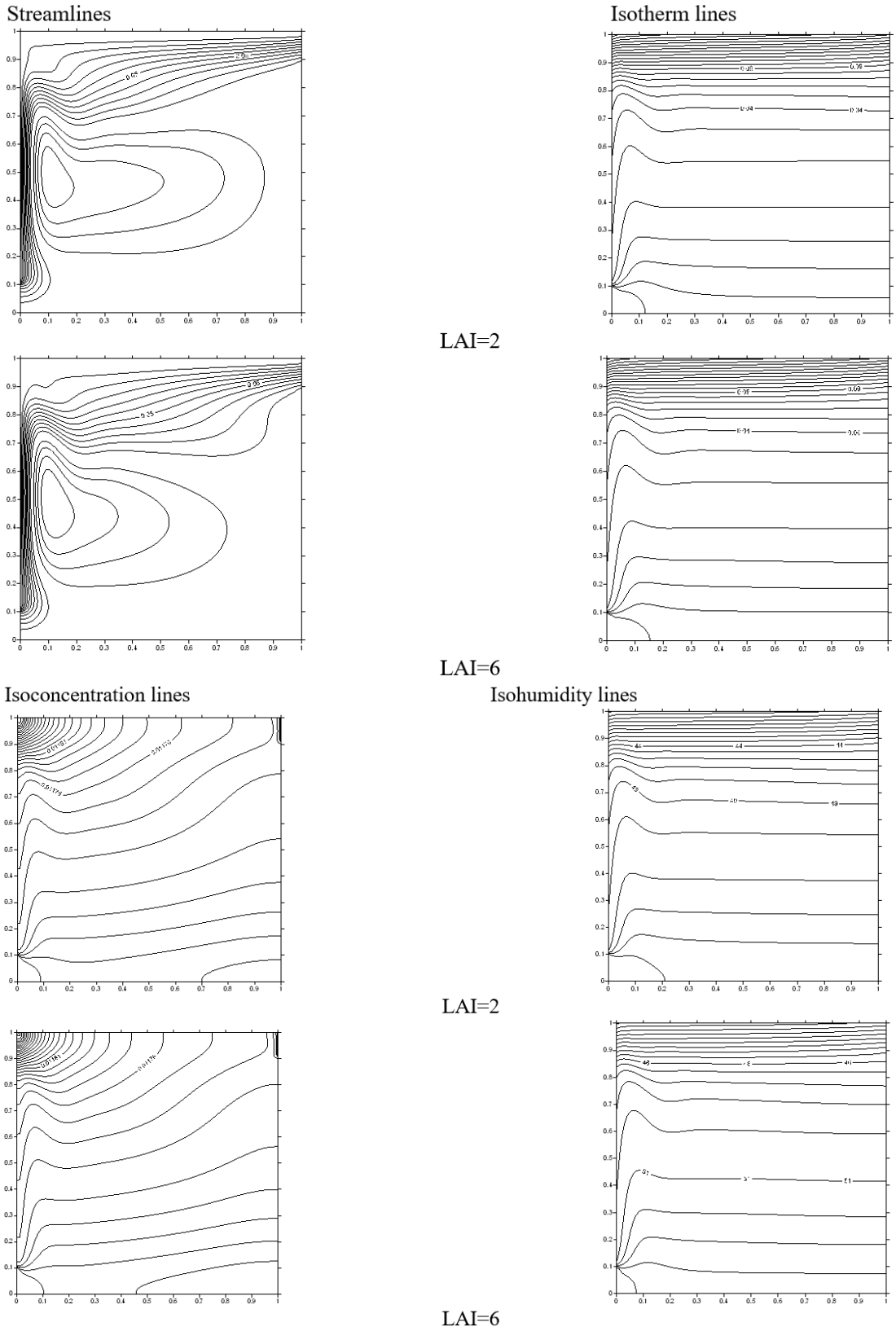

Fig. 7: (a) Streamlines and isotherm lines for ϕ = 200 W/m^2; (b) Is concentration lines and is humidity lines for ϕ = 200 W/m^2

DOI: 10.3844/ajassp.2022.6.20

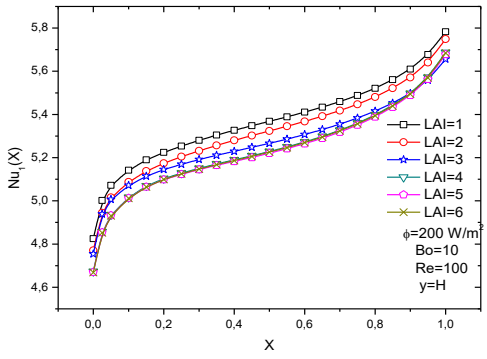

Fig. 8: Variation of local nusselt number on the top wall

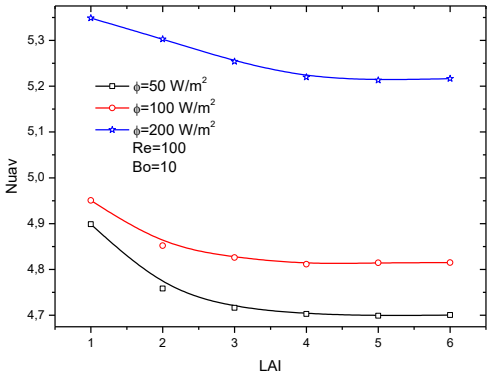

Fig. 9: Evolution of average nusselt number versus LAI

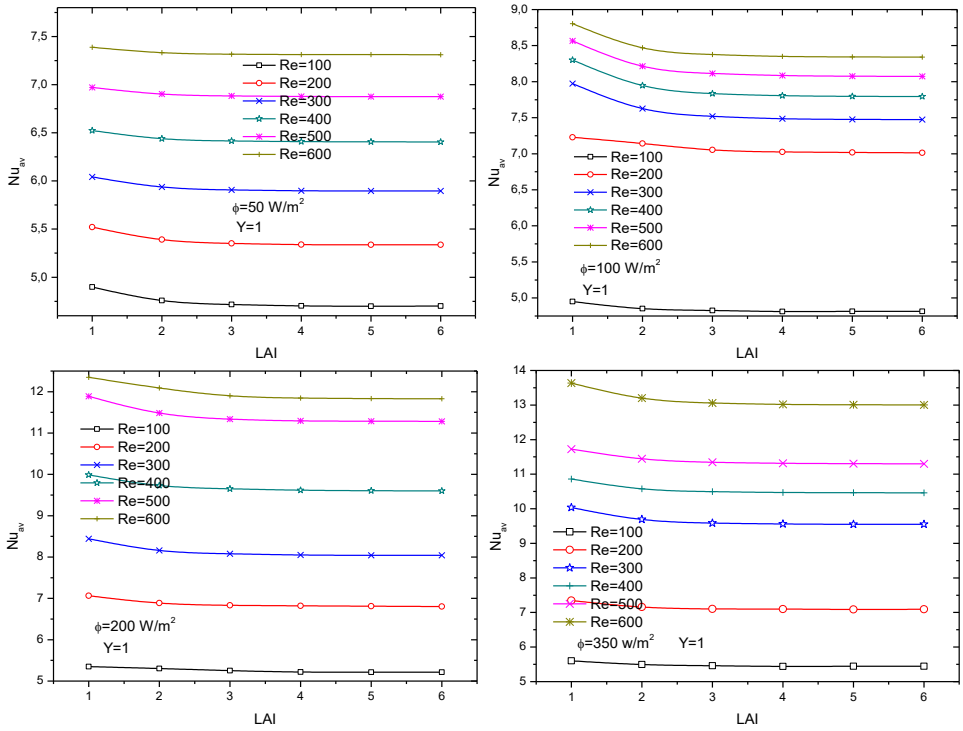

Fig. 10: Evolution of average Nusselt number versus LAI. Effect of Reynolds number. ϕ = 50 W/m2, ϕ = 100 W/m2, ϕ = 200 W/m^2 et ϕ = 350 W/m^2

Heat Transfer Correlation

It is important to know the thermal behavior of a building to facilitate the optimization of such a construction in practice. A correlation is proposed to help predict heat transfer through a green roof as a function of Reynolds number and LAI in the particular case of Lomé city (ϕ =350 W.m^{-2}). To this end, an average Nusselt number is calculated as a function of LAI and Re.

Variation of Nusselt number *Nu* as a function of the LAI for a given Re value can be calculated as:

$$Nu = A^* \exp\left(\frac{LAI}{B^*}\right) + C0^* \quad (25)$$

Table 2 presents values of coefficients A^*, B^*, and $C0^*$ for different Re values.

Re values are calculated with increments in inlet air speed to take into account natural and forced convection in the cavity. The range of Re and LAI are respectively:

$$100 \le \mathrm{R_e} \le 600 \; and \; 1 \le 1LAI \le 6.$$

The coefficients A^* and $C0^*$ given in Table 2 are correlated as a function of the Reynolds number whereas, because of its weak variation, an average value is estimated for the coefficient B^*(av = 0.88709). The agreement observed between the prediction using the correlation and numerical values are found interesting as shown in Fig. 11. The average irradiation in Lomé city is about 350 W.m^{-2} and for this reason, this value is used to propose the heat transfer correlation. The average Nusselt numbers shown in Fig. 11 are correlated in terms of the independent variables LAI and Re. The formula is given by:

$$\overline{Nu} = f(\mathrm{Re}) \exp\left(\frac{LAI}{av}\right) + g(\mathrm{Re}) \quad (26)$$

where, $g(Re)$ = 0.0145Re+4.1872:

$$f(\mathrm{Re}) = -10^{-5}\,\mathrm{Re}^2 + 0{,}0113\,\mathrm{Re} - 0{,}6568, \quad (27)$$

av = 0.08870 and the relative error not exceed 4%.

Thermal Comfort

One of the main objectives of the planted roof is to minimize the heat gains in the cavity through the roof and provide thermal comfort. This thermal comfort notion depends on the indoor air temperature and humidity. The commonly used temperature range is 22-28°C in the sub-Saharan region.

It's recommended relative humidity of 30 to 60%. The comfort temperature in ventilated room use in the present study is expressed as follows (Richard, 1997):

$$T_C = 0.48T_\alpha + 9.22 \quad (28)$$

Figure 12a and 12b are shown not only the evolution of the thermal comfort temperature versus the average outside temperature but also the effect of the leaf area index. As the LAI increases, thermal comfort temperature decreases gradually for any *Re* values. The range of comfort temperature deduced from the data is 25°C <T_c <27°. This result proves the role of the Leaf Area Index in temperature stabilization inside the cavity.

As thermal comfort is also related to air humidity, a good level of air humidity is required. To this end, the wetted wall is heated to evaporate water which could provide the appropriate humidity for inside comfort if necessary.

Figure 13 is shown the evolution of the local Nusselt number on the wetted wall for different solar heat flux density values. Local Sherwood number evolution for different solar heat flux density values is plotted in Fig. 14. Both local Nusselt and Sherwood numbers increase with solar heat flux density and showed that heat and mass transfer are proportional to solar heat flux. The intensification of water vapor transfer in the cavity increases the relative humidity as shown in Fig. 15. The range of the indoor air humidity deduced from the data is 49 to 60%. The different ranges obtained are very significant and led to the thermal comfort improvement inside the green roof's building.

Table1: Quantitative validation of the present model

Ra	Nu	Vahl Davis (1983)	Manzari (1999)	Wan *et al*. (2001)	Present study
Ra = 10^3	Max.	1.50 (0.092)	1.47 (0.109)	1.501 (0.08)	1,493 (0.09)
	Min.	0.692 (1.0)	0.623 (1.00)	0.691 (1.00)	0,637 (1.00)
	Av.	1.12	1.074	1.117	1,096
Ra = 10^4	Max.	3.53 (0.143)	3.47 (0.125)	3.579 (0.13)	3,539 (0.13)
	Min.	0.586 (1.0)	0.497 (1.0)	0.577 (1.000)	0,579 (1.00)
	Av.	2.243	2.084	2.254	2,172
Ra = 10^5	Max.	7.71(0.08)	7.71 (0.08)	7.945 (0.08)	7,758 (0.07)
	Min.	0.729 (1.0)	0.614 (1.00)	0.698 (1.00)	0,745 (1.00)
	Av.	4.52	4.3	4.598	4,431

DOI: 10.3844/ajassp.2022.6.20

Table 2: Values of coefficients A^*, B^*, and $C0^*$ for different values of Reynolds number (ϕ=*350 W.m^{-2}*)

Re	A^*	B^*	$C0^*$
100	0,47585	0,90018	5,44029
150	0,67112	0,88249	6,38125
200	0,95306	0,86584	7,09131
250	1,40243	0,88712	8,12184
300	1,69580	0,89438	9,04812
350	1,99110	0,86731	9,87815
400	1,99952	0,87999	10,46216
450	2,20922	0,88241	10,82235
500	2,19849	0,90443	11,29929
550	1,99137	0,90852	12,08145
600	2,04409	0,88534	13,00063

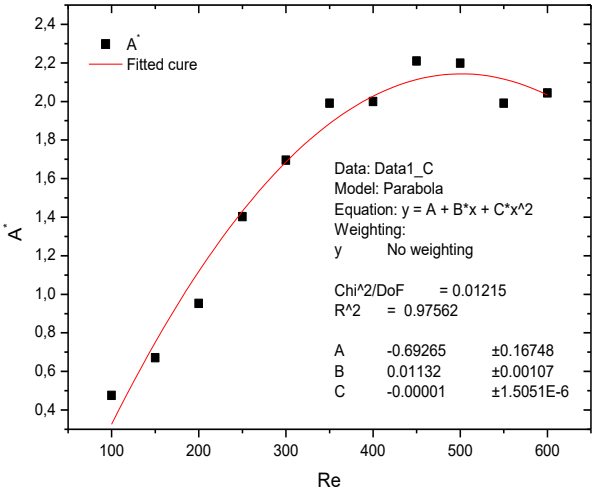

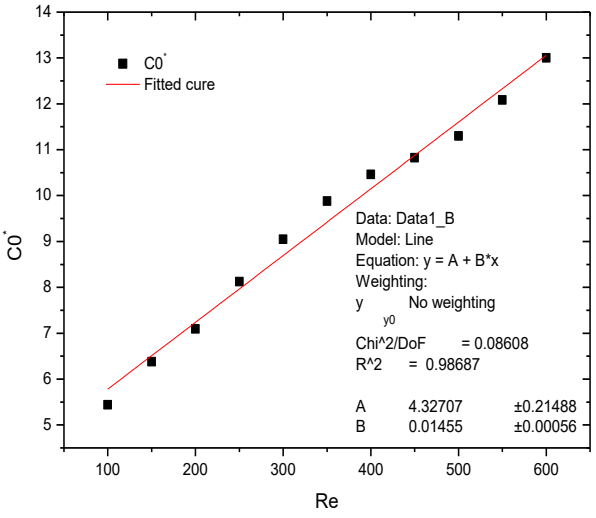

Fig. 11: Fitted curves of coefficients A^* and C_0^* as a function of Reynolds number

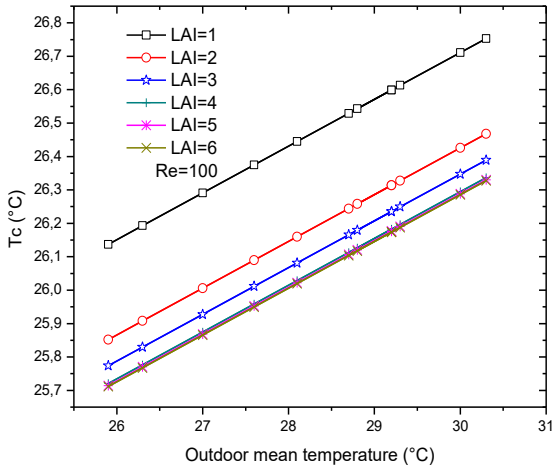

(a)

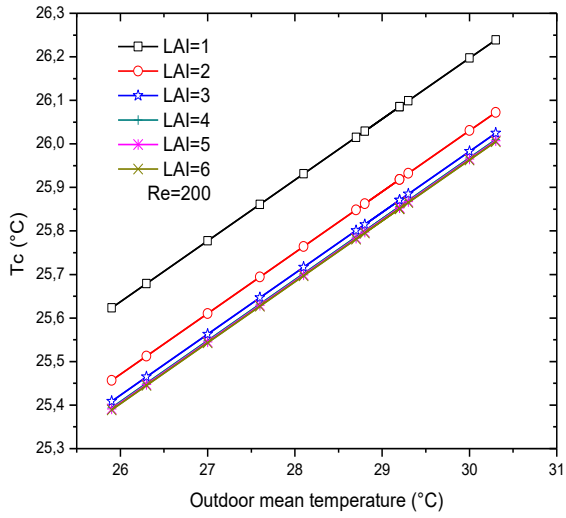

(b)

Fig.12a Evolution of the comfort temperature versus the outdoor mean temperature. (a): ϕ = 350 W.m^{-2}, Re = 100. (b): ϕ = 350 Wm^{-2}, Re = 200.

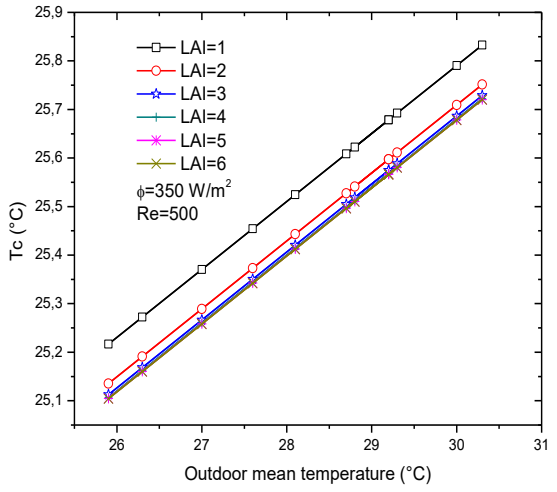

(a)

DOI: 10.3844/ajassp.2022.6.20

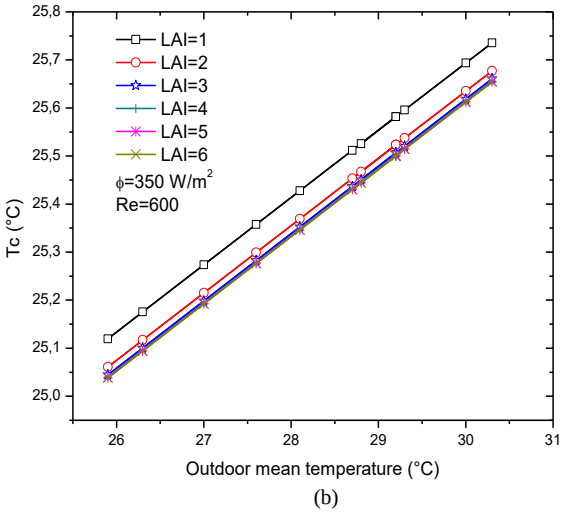

(b)

Fig. 12b: Evolution of the comfort temperature versus the outdoor mean temperature. (a): ϕ = 350 W.m^{-2}, Re = 500. (b): ϕ = 350 Wm^{-2}, Re = 600.

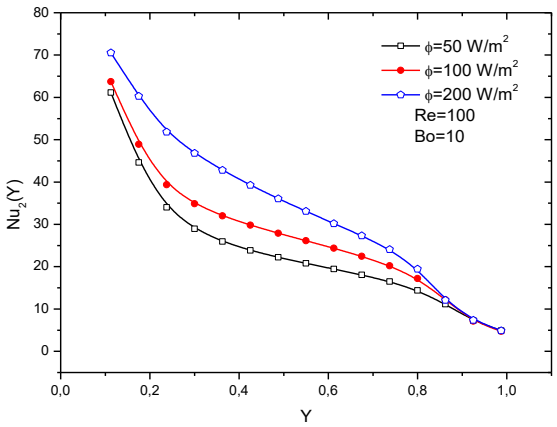

Fig. 13: Local nusselt number evolution on heated and wetted wall

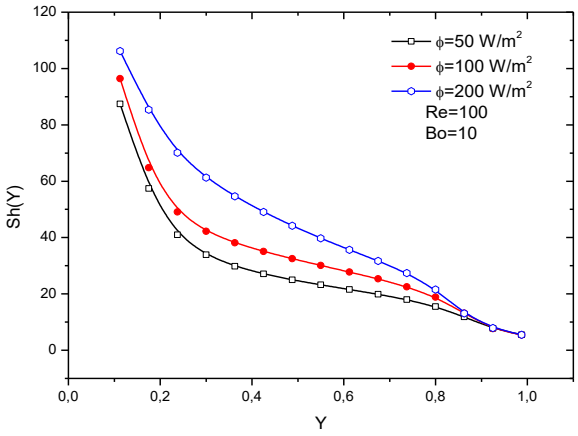

Fig. 14: Evolution of local Sherwood number on the heated and wetted wall

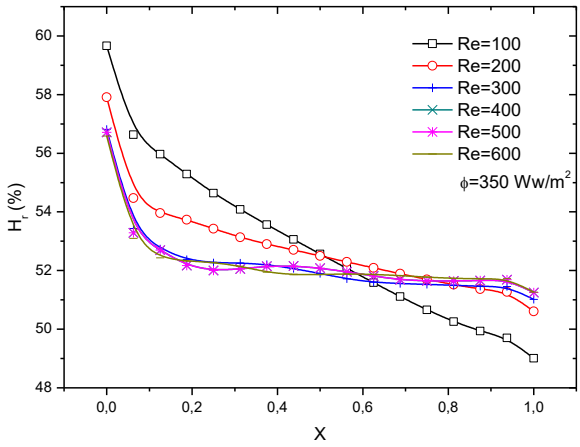

Fig. 15: Variation of average indoor air humidity in the X direction

Conclusion

A numerical investigation of the thermal comfort inside a green roof rectangular ventilated cavity in a hot and humid climate as the one of Lomé in West Africa has been done. The effects of airflow on the thermal process inside the ventilated and planted enclosure have been investigated. It was found that heat transfer in the enclosure is influenced significantly by the LAI and the ventilation in the enclosure. The comfort temperature range deduced from the data is 25°< Tc < 27° that of the indoor air humidity is: 49 % < Hr < 60%. The different ranges obtained are significant and lead to improving inside thermal comfort. The solar flux (350 W.m^{-2}) in the case of Lomé city was used to establish a heat transfer correlation to predict heat transfer through the planted roof with a relative error not exceeding 4%; so that it can be useful for engineers in the design and optimization stage of a green roof in practical buildings. A large LAI stabilizes and reduces the indoor temperature toward the acceptable range. The foliage density and therefore the plant species selection influence the thermal behavior of a green roof.

Nomenclature

α	Thermal diffusivity (m^2.s^{-1})
β_T	Thermal expansion coefficient (k^{-1})
β_c	Mass expansion coefficient (m^3.kg^{-1})
v	Kinematic viscosity(m^2.s^{-1})
p	Density (kg.m^{-3})
λ	Thermal conductivity(W.m^{-1}.k^{-1})
θ	Dimensionless temperature (-)
Ω	Dimensionless vorticity (-)
ω	Vorticity (s^{-1})
Ψ	Dimensionless stream function (-)
ψ	Stream function (m^2.s^{-1})

ζ	ratio of the heat transmitted to the wetted wall
τ	Dimensionless time (-)
BO	Biot number (-)
C^*	Dimensionless concentration (-)
C	Concentration ($kg.m^{-3}$)
D	mass diffusivity
e	size of inlet and outlet (m)
g	gravitational acceleration ($m.s^{-2}$)
G_{rT}	Thermal Grashof number (-)
G_{rS}	Solutal Grashof number (-)
H	height of the cavity (m)
H_r	Relative humidity (%)
L	width of the cavity (m)
Lv	Latent heat of water vaporization ($j.kg^{-1}$)
LAI	Leaf Area Index (-)
n	outward normal direction/iteration in a loop
$N_u(X)$	Local Nusselt number (-)
$N_u(Y)$	Local Nusselt number (-)
Nu_{av}	average Nusselt number (-)
Pr	Prandtl number (-)
Pv	Vapour pressure (P_a)
P_{vs}	Saturated vapour pressure (P_a)
Φ	Average solar heat flux ($W.m^{-2}$)
R_e	Reynolds number (-)
R_{iT}	Thermal Richardson number (-)
R_{iS}	Solutal Richardson number (-)
$S_h(Y)$	Local Sherwood number (-)
FE	Solar Heat gain Factor (-)
T_c	Comfort temperature (k or °C)
T_i	Inside average temperature (k or °C)
T_a	Ambient temperature (k or °C)
t	Time (s)
U, V	Dimensionless velocity components (-)
u, v	Velocity components ($m.s^{-2}$)
u_0	Inlet air velocity ($m.s^{-1}$)
X, Y	Dimensionless coordinate (-)
x, y	Cartesian coordinate (m)

Acknowledgment

The authors thank LES/GPTE of the University of Lomé and LAMPS/GME of the University of Perpignan via Domitia for their favorable research environment.

Study Limitations

- This study is be based on a model simulation of a green roof building in the West African context
- The study does not provide detailed modeling of the green roof but uses the results of previous studies by the authors themselves as input data for the current model
- The study does not analyze the life cycle analysis, costs, and social benefits of green roof
- The study does not analyze the potential of the green roof to mitigate the heat island effect and greenhouse gas mitigation in the urban areas

Author's Contribution

Hodo-Abalo Samah: Contributions in the physical model definition, writing model equations, simulating the model, analyzing and interpreting results. Write the draft of the article. Give final approval of the version to be submitted and any revised version.

Magolmèèna Banna and Belkacem Zeghmati: Contributions in the physical model definition, corrects equations, supervises model simulation, analysis and interprets results. Corrects the draft of the article and contributes significant intellectual content. Give final approval of the version to be submitted and any revised version.

Ethics

The authors declare that they have no known competing financial interests or personal relationships that could have appeared to influence the work reported in this study. This article is original and contains an unpublished study. The corresponding author confirms that all of the other authors have read and approved the manuscript and no ethical issues.

References

Angirasa, D. (2000). Mixed convection in a vented enclosure with an isothermal vertical surface. *Fluid Dynamics Research*, 26(4), 219.

Banna, M., Zeghmati, B., & Bresson, J. (2002). Diurnal heat and water vapor exchange in vegetation canopy in an area of high solar radiation. *International Journal of Energy, Environment and Economics*, 11, 143-163. doi.org/10.1016/S0169-5983 (99) 00024-6.

Del Barrio, E. P. (1998). Analysis of the green roofs cooling potential in buildings. *Energy and Buildings*, 27(2), 179-193. doi.org/10.1016/S0378-7788(97)00029-7.

Dong, J., Lin, M., Zuo, J., Lin, T., Liu, J., Sun, C., & Luo, J. (2020). Quantitative study on the cooling effect of green roofs in a high-density urban Area-a case study of Xiamen, China. *Journal of Cleaner Production*, 255, 120152. doi.org/10.1016/j.jclepro.2020.120152.

Hodo-Abalo, S., Banna, M., & Zeghmati, B. (2012). Performance analysis of a planted roof as a passive cooling technique in hot-humid tropics. *Renewable Energy*, 39(1), 140-148. doi.org/10.1016/j.renene.2011.07.029

Jamei, E., Chau, H. W., Seyedmahmoudian, M., & Stojcevski, A. (2021). Review the cooling potential of green roofs in different climates. *Science of The Total Environment*, 148407. doi.org/10.1016/j.scitotenv.2021.148407

Jain, D. (2006). Modeling of solar passive techniques for roof cooling in arid regions. *Building and Environment*, 41(3), 277-287. doi.org/10.1016/j.buildenv.2005.01.023

Joseph K. S. (1999). Typological study of the solar collection of buildings in humid tropical regions. Unpublished Ph.D. dissertation in French language, Institut Polytechnique de Grenoble.

Kumar, R., & Kaushik, S. C. (2005). Performance evaluation of green roof and shading for thermal protection of buildings. *Building and Environment*, 40(11), 1505-1511. doi.org/10.1016/j.buildenv.2004.11.015

Lee, K.T., Tsai, H.L., & Yan, W.M. (1997). Mixed convection heat and mass transfer in vertical rectangular ducts. *International Journal of Heat and Mass Transfer*, 40(7), 1621-1631. doi.org/10.1016/S0017-9310(96)00192-5

Manzari, M. T. (1999). An explicit finite element algorithm for convection heat transfer problems. *International Journal of Numerical Methods for Heat and Fluid Flow*. doi.org/10.1108/09615539910297932

Nahar, N. M., Sharma, P., & Purohit, M. M. (1999). Studies on solar passive cooling techniques for arid areas. *Energy Conversion and Management*, 40(1), 89-95. doi.org/10.1016/S0196-8904(98)00039-9

Raji, A., & Hasnaoui, M. (1998). Mixed convection heat transfer in a rectangular cavity ventilated and heated from the side. *Numerical Heat Transfer, Part A Applications*, 33(5), 533-548. doi.org/10.1080/10407789808913953

Raji, A., & Hasnaoui, M. (2000). Mixed convection heat transfer in ventilated cavities with opposing and assisting flows. *Engineering Computations*. doi.org/10.1108/02644400010339770

Richard, D. (1997). Developing an adaptive model of thermal comfort and preference. Final Report ASHRAE RP 884.

Saha, S., Hasan, M. N., & Khan, I. A. (2009). Double diffusive mixed convection heat transfer inside a vented square cavity. *Chemical Engineering Research Bulletin*, 13(1), 17-24. doi.org/10.3329/cerb.v13i1.2512

Sailor, D. J., Hutchinson, D., & Bokovoy, L. (2008). Thermal property measurements for Eco roof soils are common in the western US. *Energy and Buildings*, 40(7), 1246-1251. doi.org/10.1016/j.enbuild.2007.11.004

Samah, H. A., & Banna, M. (2009). Performance analysis of thermal insulation screens used for classic roofs in hot-humid tropics. *International Energy Journal*, 10(4). http://203.159.5.126/index.php/reric/article/view/670

Samah, H. A., Tiwari, G. N., & Nougbléga, Y. (2020). Cool and Green Roofs as Techniques to Overcome Heating in Building and its Surroundings under Warm Climate. *International Energy Journal*, 20(3). https://www.thaiscience.info/Journals/Article/IENJ/10992380.pdf

Tang, R., & Etzion, Y. (2004). On the thermal performance of an improved roof pond for cooling buildings. *Building and Environment*, 39(2), 201-209. doi.org/10.1016/j.buildenv.2003.09.005

Tiwari, G. N. (2002). Solar energy: Fundamentals, design, modeling, and applications. Alpha Science Int'l Ltd.

Vahl Davis D. (1983). Natural convection of air in a square cavity: A Bench Mark Solution. *Int. J. Numer. Fluids*, 3, 249-264.

Wan, C., Patnaik, B. S. V., Wei, G. W. D. (2001). A new benchmark quality solution for the buoyancy-driven cavity by discrete singular convolution. *Numerical Heat Transfer: Part B: Fundamentals*, 40(3), 199-228. doi.org/10.1080/104077901752379620

Wong, N. H., Chen, Y., Ong, C. L., & Sia, A. (2003). Investigation of thermal benefits of rooftop garden in the tropical environment. *Building and Environment*, 38(2), 261-270. doi.org/10.1016/S0360-1323(02)00066-5

Yan, W. M. (1996). Combined buoyancy effects of thermal and mass diffusion on laminar forced convection in a horizontal rectangle.